"WETTING BY SOLID STATE" GRAIN BOUNDARY PHASE TRANSITION IN Zn–Al ALLOYS

B.B. Straumal[1], A.S. Khruzhcheva[1] and G. A. López[2]

[1]Institute of Solid State Physics, Russian Academy of Sciences, Chernogolovka, Moscow distr., 142432, Russia
[2]Max-Planck-Institut für Metallforschung, Heisenbergstrasse 3, D-70569 Stuttgart, Germany

Abstract. The microstructure of Zn–5wt.%Al polycrystals has been studied between 250 and 375 °C. The evolution of continuous (Al) layers at individual Zn grain boundaries (GBs) has been studiet at 230 and 290 °C. The (Al) phase forms either chains of separated lens-like precipitates or continuous uniform layers at (Zn) GBs. If the GB particles are observed, the contact angle q>0? at the intersection between (Al)/(Zn) interphase boundaries (IBs) and (Zn)/(Zn) GB. With increasing temperature q becomes zero at certain T_{ws} and remains zero above T_{ws}. Above T_{ws} a (Zn) GB is covered by continuous (Al) layer. T_{ws} inversely correlates with the GB energy. The fraction of (Zn) GBs covered by (Al) layers increases with increasing temperature. Therefore, the GB phase transition 'wetting by solid phase' proceeds in Zn–Al alloys. It is thermodynamically similar to the GB wetting phase transition by liquid phase. The tie-line of a GB phase transition is constructed in the conventional bulk Zn–Al phase diagram. Such GB tie-lines are especially important for the nanocrystalline materials.

1. INTRODUCTION

One of most important processes in the heat treatment of materials is the decomposition of supersaturated solid solutions. The morphology of decomposition products strongly influences the properties of a material. The heterogeneous nucleation of a new phase at a grain boundary (GB) proceeds easier than the homogeneous one in the supersaturated matrix [1,2]. It is just due to the fact that when a particle of a new phase with radius r nucleates and grows at a GB, it cuts out a GB circle with an area of πr^2. As a result it leads to an energy gain of $\sigma_{GB} \pi r^2$ (σ_{GB} being the GB free energy per unit area) in comparison to the homogeneous nucleation. If we consider the fully relaxed state (neglecting the influence of internals stresses appeared during nucleation and growth of a new phase), two principally different morphologies of second phase particles are possible at a GB.

(1) The GB energy $\sigma_{GB}^{\alpha\alpha}$ in the matrix α is lower than the energy $2\sigma_{IB}^{\alpha\beta}$ of two interphase α/β boundaries (IB) between growing β-particle and super-saturated α-matrix (Fig. 1d). In this case the growing b-particle has a lens-like shape and forms an equilibrium contact angle θ along the contact line between IBs and GB. The q value is given by the condition of mechanical equilibrium $\sigma_{GB}^{\alpha\alpha} = 2\sigma_{IB}^{\alpha\beta} \cos(\theta/2)$.

(2) If $\sigma_{GB}^{\alpha\alpha} > 2\sigma_{IB}^{\alpha\beta}$ the α/α GB is unstable in the contact with growing β-phase, equilibrium contact angle $\theta = 0$ and the layer of β-phase has to cover continuously the a/a GB (Fig. 1e).

The facts (1) and (2) seem to be trivial. Particularly, the layers of second phase fully covering the GBs in a matrix were observed in many systems. Just most important examples are the Fe_3C layers at the ferrite and austenite GBs in steels [1, 2], GB layers of Cu in sintered W polycrystals [3–8], β-(Zr,Nb) layers in GBs of α-Zr [9] or Bi layers between Cu grains [10]. The continuous GB layers of a second phase can be either detrimental (like brittle GB cementite in steels or Bi-layers in Cu alloys) or favourable like Cu layers improving plasticity of W polycrystals.

Corresponding author: B.B. Straumal, e-mail: straumal@issp.ac.ru
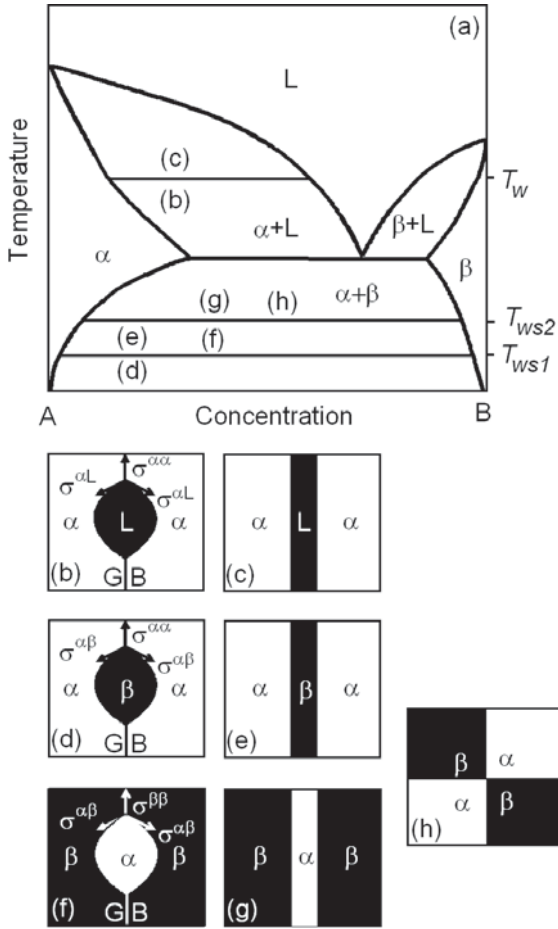
Fig. 1. (a) Schematic phase diagram showing tie-lines of GB wetting by a liquid phase and of GB wetting by a solid phase at T_w, and T_{ws1} and T_{ws2}, respectively. (b) Liquid phase L does not wet a GB in the solid phase α ($T < T_w$). (c) Liquid phase L wets a GB in the solid phase α ($T > T_w$). (d) Solid phase β does not wet a GB in the solid phase a?($T < T_{ws1}$). (e) Solid phase β wets a GB in the solid phase α ($T > T_{ws1}$). (f) Only α/β IBs exist in an $\alpha+\beta$ polycrystal if wetting occurs at both α/α and β/β GBs ($T > T_{ws2}$).

Situation with complete and incomplete GB wetting (covering) by the layer of second solid phase is very similar to the conventional GB wetting phase transition by liquid phase which has been well studied recently [11–25]. If the GB energy $\sigma_{GB}^{\alpha\alpha}$ is lower than the energy of two solid/liquid interfaces $2\sigma_{IB}^{\alpha\beta}$, the GB is not completely wetted and the contact angle $\theta > 0$ (Fig. 1b). If $\sigma_{GB}^{\alpha\alpha} > 2\sigma_{IB}^{\alpha\beta}$ the GB is wetted completely by the liquid phase and $\theta = 0$ (Fig. 1c). If the temperature dependences $\sigma_{GB}^{\alpha\alpha}(T)$ and $2\sigma_{IB}^{\alpha\beta}(T)$ intersect, then the GB wetting phase transition proceeds at the temperature T_w of their intersection.

The contact angle θ decreases gradually with increasing temperature down to $\theta = 0$ at T_w. Above T_w the contact angle remains $\theta = 0$ (Fig. 1c). The *tie-line of the GB wetting phase transition* appears at T_w in the two-phase region ($\alpha+L$) of the bulk phase diagram (Fig. 1a). Above this tie line GBs with an energy $\sigma_{GB}^{\alpha\alpha}$ cannot exist in equilibrium with the liquid phase. The liquid phase forms a layer separating the crystals. T_w depends on the GB energy. GBs with lower energy possess higher T_w [16]. In polycrystals the whole spectrum of GBs with various energies exists. Therefore, in polycrystals the maximal T_{wmax} and minimal T_{wmin} can be found for high-angle GBs with minimal and maximal energy $\sigma_{GB\,min}^{\alpha\alpha}$ and $\sigma_{GB\,max}^{\alpha\alpha}$, respectively. The tie-lines at T_{wmax} and T_{wmin} have been constructed in the Al–Mg, Al–Zn and Al–Sn bulk phase diagrams [16, 22–25]. Above T_{wmax} all GBs are completely wetted. At the temperatures between T_{wmax} and T_{wmin} some GBs are wetted by the liquid phase and other GBs are not wetted. Below T_{wmin} all GBs are not wetted, and the melt has a shape of separated inclusions. With increasing temperature between T_{wmin} and T_{wmax} the fraction of the wetted GBs increases from 0 at T_{wmin} to 100% at T_{wmax} [10, 22–25]. From the obvious thermodynamic similarity between conventional GB wetting by liquid phase and GB wetting (covering) by solid phase several phenomena can be predicted. They have not been observed before to the best of our knowledge:

- Transition from the incomplete GB wetting (covering) by second solid phase to the complete GB wetting (covering) with increasing temperature at certain T_{ws};
- Dependence of T_{ws} on the GB energy (low T_{ws} for high $\sigma_{GB}^{\alpha\alpha}$ and vise versa);
- Appearance of new tie-lines of 'wetting by solid phase' GB phase transitions in a $\alpha+\beta$ two-phase area of the conventional bulk phase diagrams where two solid phases α and β are in equilibrium between T_{wsmax} and T_{wsmin};
- Increase of portion of GBs covered by solid phase from 0 to 100% with temperature increasing from T_{wsmin} to T_{wsmax}.

In order to observe these phenomena we have chosen the Al–Zn system. The conventional GB wetting phase transition proceeds in the two-phase (Al)+*L* area of the Al–Zn phase diagram [23,25]. By investigation of GB wetting we observed the indications of the GB wetting by solid phase in the Zn-reach alloys and continued to investigate this phenomenon. The results of this study are presented below.
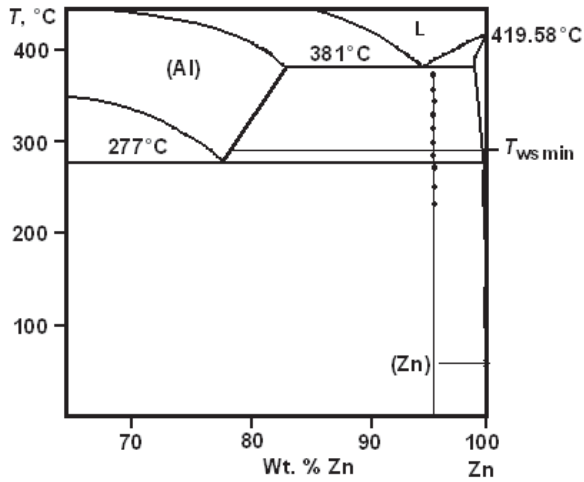
Fig. 2. The Zn–Al equilibrium phase diagram [26]. The vertical thin line represents the Zn–5wt.%Al alloy of this study. Points at that line represent the annealing temperatures applied. The tie-line at T_{wsmin} ≈ 290 °C represents the minimal temperature determined in this work for wetting of Zn-rich phase/Zn-rich phase GBs by the Al-rich phase.

2. EXPERIMENTAL

A Zn–5wt.%Al alloy was prepared by vacuum ($P = 10^{-5}$ Pa) induction melting and casting into 9 mm diameter rods. It was made of high purity Zn (99.999 wt.%) and Al (99.9995 wt.%). The 2 mm thick disks were prepared from the alloy buttons by grinding, spark erosion, sawing and chemical etching for 15 s in fluorhydric acid. The polycrystalline samples were then encapsulated in evacuated ($<4 \cdot 10^{-4}$ Pa) quartz glass tubes and annealed in a tube furnace maintained within ± 2°C at several temperatures between 250 °C and 375 °C (see Fig. 2) for 336, 672 and 2016 h.

Zn bicrystals with symmetric tilt [1,1,–2,0] GBs with misorientation angles of 46° and 84° were grown from Zn of 99.999 wt.% purity using the directed crystallization method. The orientation of single crystal seeds and the orientation of the crystallographic axes of the bicrystals were controlled using Laue back reflection. The misorientations of grains in bicrystals were also defined by the measuring of the misorientations of [1000] cleavage bands on the surface of both grains using optical microscope after cleavage of bicrystals in liquid nitrogen. The flat bicrystals having dimensions 1x10x120 mm with the flat GB laying parallel to the long axis and perpendicular to the (1,1,–2,0) surface were grown in high purity graphite crucibles in the atmosphere of high
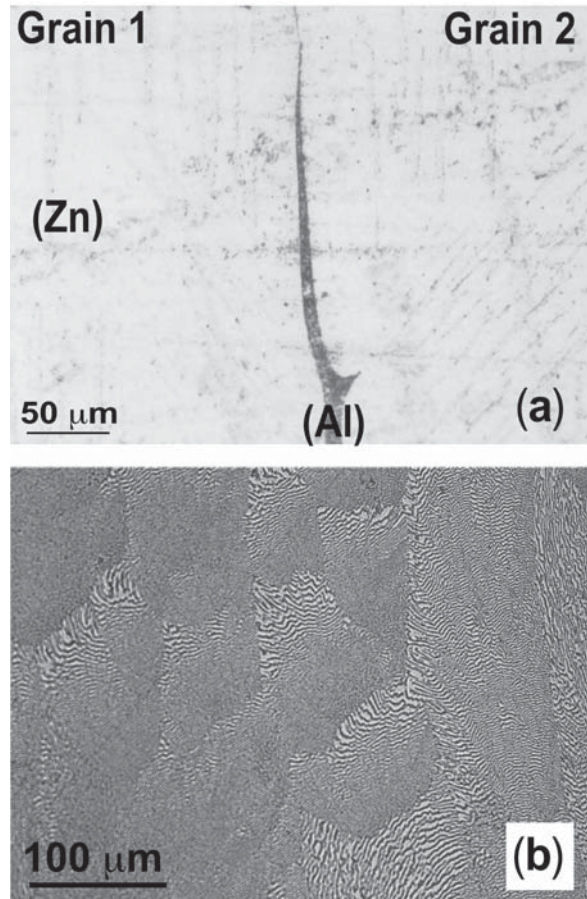
Fig. 3. (a) The continuous layer of (Al) phase at the Zn tilt GB in [1,1,–2,0] bicrystal formed after annealing at 415 °C. The contact angle between liquid (Al) phase and GB in solid Zn phase at is very close to zero. (b) Optical micrograph of cross-section of the as-cast Zn–5wt.%Al alloy after melting and cooling down to room temperature.

purity argon (with oxygen concentration equivalent to the vacuum of 10^{-5} Pa). After growing the bicrystals were cut by spark erosion as 20 mm long pieces. For the wetting experiments the samples with the (Al) layer were then produced. For this purpose the Zn bicrystals were etched for few seconds in pure HNO_3 acid and brought in contact with liquid Al of 99.999 wt.% purity at about 390 °C in an apparatus made from high purity graphite. The surface layer at the end of the Zn bicrystal dissolves in the liquid Al and saturates the melt up to liquidus concentration at 390 °C. The contact between the melted Zn(Al) and the Zn bicrystal forms within a few seconds. Then the apparatus was cooled down and the (Al)-coated Zn sample was cut by spark erosion. The samples were 10–13 mm long with 0.2–0.4 mm thick Sn layers. The ratios between length of Zn bicrystal and thickness of Al-rich layer were selected so that

the average sample composition during the subsequent anneal was in the two-phase field of the Al–Sn phase diagram [26]. The bicrystalline samples were then encapsulated in evacuated (<4 10⁻⁴ Pa) quartz glass tubes and annealed about 30 min in a tube furnace maintained within $\pm$2°C at 415 °C. This temperature is above the GB wetting phase transition temperature of Zn GBs by (Al) liquid phase. As a result the continuous layer of (Al) phase was build in Zn GBs (Fig. 3a). The quartz glass tubes were that quenched in air without breaking the vacuum. The Zn bicrystals with GB covered by continuous layer of (Al) phase were than annealed once again at 230 and 290 °C for 480 h.

After quenching in water, the microstructures of the polycrystalline and bicrystalline specimens were studied by optical microscopy and scanning electron microscopy (SEM). For the investigations the samples were etched for 15 s in fluorhydric acid. To confirm the presence of the different phases X-ray diffraction (XRD) patterns were acquired from the bulk samples. XRD data were obtained on the SIEMENS–500 diffractometer with a graphite monochromator and line position sensitive gas flow detector. Cu $K_{\alpha 1}$ radiation was used. Electron probe microanalysis (EPMA) measurements were carried out by wavelength dispersive analysis on a JEOL 6400 electron probe microanalyser operated at 15 kV. For the determination of the concentration profiles the beam was stepped at 1 to 5 μm intervals. Electron back scattering (EBS) measurements were carried out in a scanning regime on a JEOL 100CX electron microscope operated at 100 kV.

3. RESULTS

In Fig. 3b the microstructure of Zn–5 wt.%Al alloy after solidification and cooling is shown. This structure represents the starting ('as-casted') state of our samples before long anneals for investigations of GB solid state wetting (covering) phase transformations. It contains the eutectic colonies of (Al) and (Zn) lamellae formed at eutectic temperature T_e= 381 °C during solidification. Similar eutectic mixture replaces the liquid (Al) layer at Zn GBs in bicrystals during the cooling down from the annealing temperature of 415 °C (Fig. 3a). Since the composition of studied alloy is very close to the eutectic one, almost no (Al) or (Zn) primary crystals are present in the microstructure of the Zn–5wt.% Al polycrystal. The volume fraction of (Zn)-phase in the eutectic is higher than that of (Al) in correspondence with the phase diagram and specific densities of both phases. Therefore, each eutectic colony can

be regarded as a (Zn) grain containing (Al) lamellae. The neighbouring eutectic colonies form (Zn)/(Zn) GBs. No (Al)/(Al) GBs as colony boundaries can be observed in the starting state. The (Al)/(Al) GBs are present only locally, in the points of occasional contacts between (Al) lamellae in the neighbouring eutectic colonies. For our investigations it is important to observe, that the (Al) lamellae in each colony [i.e. (Zn) grain] start (or finish) at the boundaries between colonies [i.e. (Zn)(Zn) GBs] independently from (Al) lamellae in a neighbouring colony. The (Zn)/(Zn) GBs do not have neither continuous (Al) layers or chains of (Al) (Fig. 3b). The (Al) lamellae in neighbouring eutectic colonies meet at the (Zn)/(Zn) GBs as a kind of two combs or brushes. During the cooling to the room temperature, the second (monotectoid) transformation proceeds at T_{mt} = 277 °C in (Al) lamellae. The (Al) solid solution with Al content of about 18 wt.% decomposes into two (Al) solid solutions with Al content of about 22 wt.% and 35 wt.%. This fine structure of former eutectic (Al) lamellae can be seen in Figs. 4c and 5a.

The starting microstructure changes after long anneals at several temperatures between 250 and 375 °C. In Fig. 4 the typical microstructure of Zn–5wt.%Al alloys annealed for annealed for 2160 h at 275 °C (Fig. 4a), 720 h at 375 °C (Fig. 4b) 2160 h at 375 °C (Fig. 4c) and 2160 h at 275 °C (Fig. 4d) is presented. In all samples the (Al) lamellae in the bulk coarsen and retard from the (Zn)/(Zn) colony boundaries. The (Al) precipitates start to grow at the previously precipitate-free (Zn) GBs. Two different kinds of precipitate morphologies have been observed at the (Zn)/(Zn) GBs. First, the GB chains of isolated (Al) precipitates like those shown in Fig. 4a and d were seen. Second, the occurrence of a continuous solid (Al) layer covering certain (Zn)/(Zn) GBs were clearly visible (Fig. 4b and c). In Fig. 4c the triple junction of (Zn)/(Zn) GBs is shown. The GBs are fully covered by thick and uniform (Al) layer. With increasing annealing time all kinds of (Al) precipitates coarsen. The coarsening is more pronounced at higher temperatures. The (Al) lamellae in the bulk become unstable, broke and start to spheroidize. The GB individual precipitates remain lens-like and also coarsen. In the contrary, the continuous GB layers of Al remain flat and become thicker and thicker with increasing annealing time. These facts demonstrate that the GB wetting by solid phase (covering) phase transition proceeds in the (Al)+(Zn) two-phase eutectic area of the Zn–Al bulk phase diagram. The primarily precipitate-free (Zn) GBs in the presence of (Al) phase separate
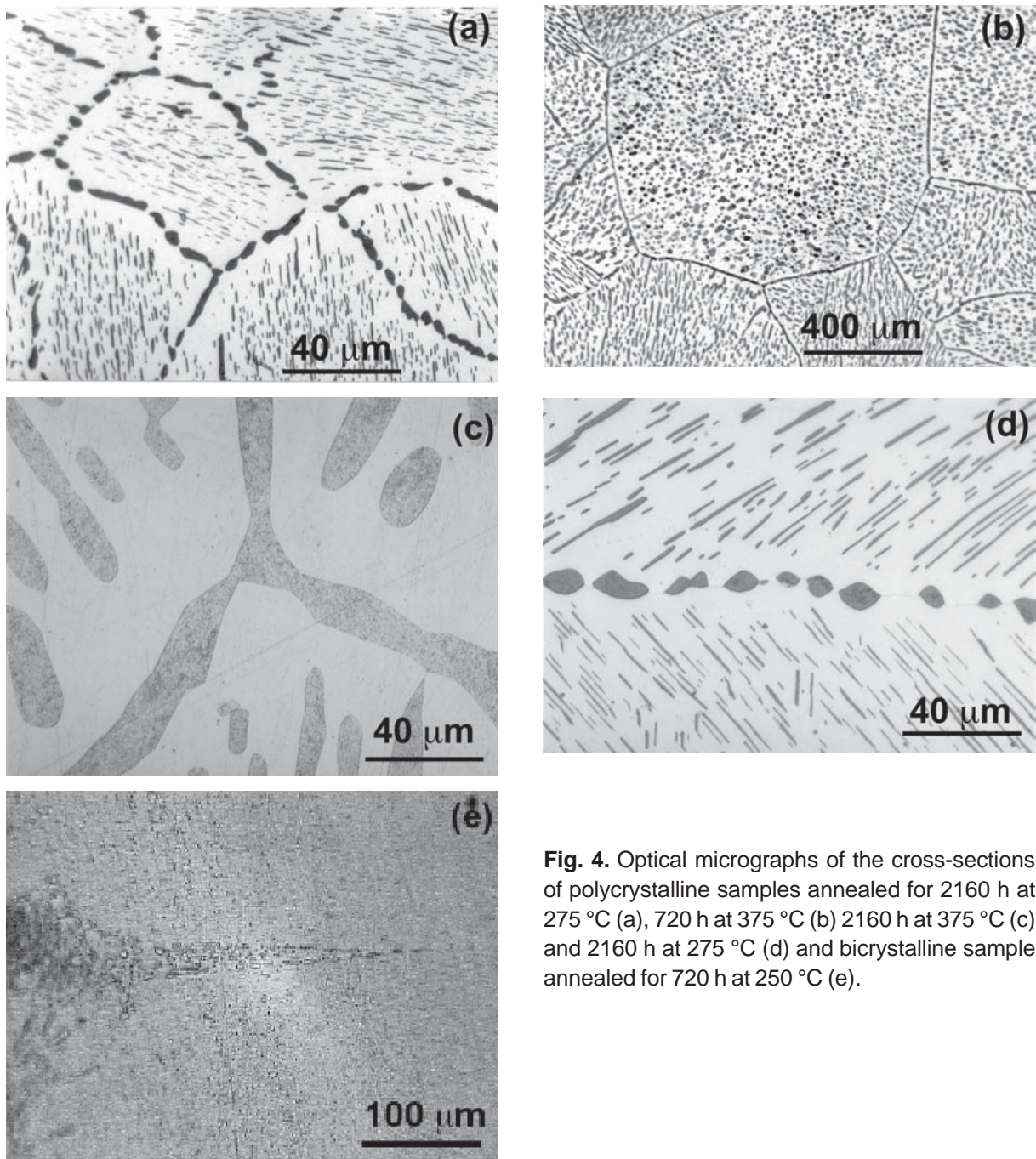
Fig. 4. Optical micrographs of the cross-sections of polycrystalline samples annealed for 2160 h at 275 °C (a), 720 h at 375 °C (b) 2160 h at 375 °C (c) and 2160 h at 275 °C (d) and bicrystalline sample annealed for 720 h at 250 °C (e).

into two groups. In the GBs of the first group the chains of (Al) precipitates develop. These (Al) particles are separated by the intact portions of a (Zn)/(Zn) GB. In the GBs of the second group the continuous and macroscopically thick flat layers of (Al) develop. With increasing time the morphology of GB precipitates change only quantitatively (particles coarsen and layers thicken), but not qualitatively. In Fig. 4e the microstructure of individual GB is shown after annealing for 720 h at 250 °C. The continuous

(Al) GB layer decomposes after this annealing into separated droplets, similar to those in polycrystalline samples.

The compositions of the phases involved were confirmed by electron probe microanalysis (Fig. 5). The average composition of the (Zn) solid solution (0.91 wt.% Al) as well as that of the (Al) solid solution (21.9 wt.% Al), which after quenching de-composes according to a monotectoid reaction, corresponds well with the equilibrium values at this tem-
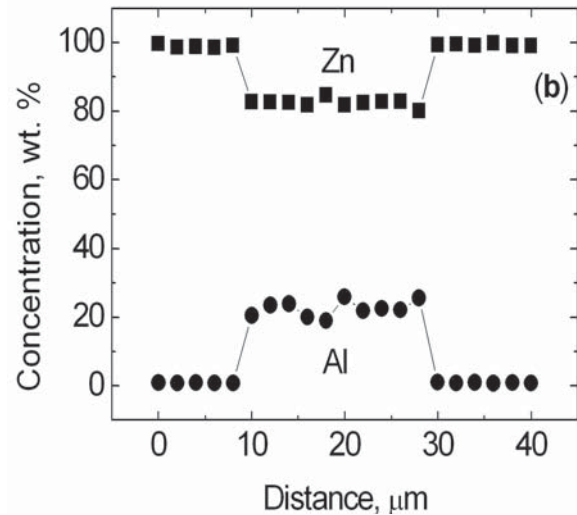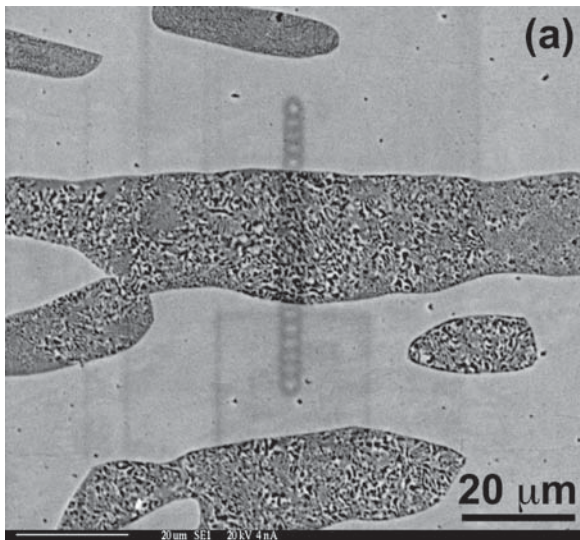
Fig. 5. Secondary-electron micrograph of a specimen annealed at 345 °C for 2160 h (a). Composition profile along the line indicated in the micrograph as determined by EPMA (b).

perature. The analysis line intersects the GB layer formed at a (Zn)/(Zn) GB. The fine structure of the monotectoid mixture appeared during the quenching in the (Al) GB layers and coarsened bulk lamellae are clearly visible.

The number of GBs either covered by continuous layers of (Al) solid phase or containing the chain of (Al) particles has been counted at each annealing temperature for about 100 GBs, and the respective ratio has been measured. In Fig. 6 the temperature dependence of the fraction of (Zn) GBs covered by continuous layers of (Al) solid phase is shown. The temperatures T_{mt} and T_e of the bulk monotectoid and eutectic transformations are marked. Below T_{mt} all GBs are not covered by solid phase. Still at $T=$ 283 °C, i.e. above T_{mt}, all (Zn) GBs contain only chains of (Al) particles. At 300 °C first (Zn) GBs completely covered by continuous layers of (Al) solid phase appear in the samples. It means that the minimal temperature of GB 'wetting by solid phase' (covering) transformation T_{wsmin} for (Zn) GBs lies between 283 and 300 °C. Respective tie-line for the minimal temperature T_{wsmin} of GB covering (wetting by solid phase) phase transformation has been drown in the two-phase (Al)+(Zn) area of the conventional bulk Zn–Al phase diagram (Fig. 2). The fraction of covered (Zn) GBs increases with increasing temperature, similar to the fraction of GBs wetted by liquid phase between T_{wmin} to 100% at T_{wmax} [10, 22–25]. However, the fraction of covered (Zn) GBs does not reach 100%. Just below eutectic tempera-

ture T_e only about 35% of (Zn) GBs are fully covered by continuous layer of (Al) solid phase. It means that $T_{wmax} > T_e$ for the GB 'wetting by solid phase' (covering) transformation, and no T_{wmax} line of complete "wetting by solid phase" for (Zn) GBs appears in the (Al)+(Zn) area of the conventional bulk Zn–Al
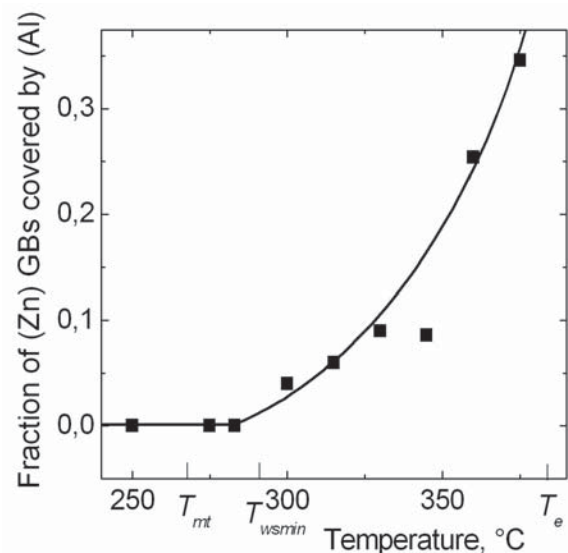
Fig. 6. Temperature dependence of the fraction of Zn-rich phase/Zn-rich phase GBs fully wetted by a continuous layer of the Al-rich phase. The temperatures T_{mt} and T_e of the bulk monotectoid and eutectic transformations have been indicated. T_{wsmin} is the minimal temperature of GB wetting by a solid phase.
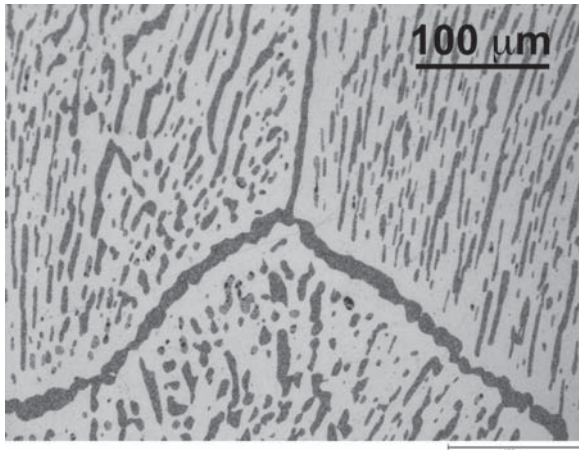
Fig. 7. Optical micrograph of the cross-section of samples annealed for 336 h at 250 °C (a), and than for 48 h at 370 °C. The GB chains of (Al) particles formed after first annealing grew together after second one.

phase diagram (Fig. 2). Such GB tie-lines are especially important for the nanocrystalline materials.

4. DISCUSSION

If the phenomenon observed in the Zn–5 wt.%Al alloys is really an equilibrium GB phase transition, the fraction of covered (Zn) GBs shall depend only on the crystallographic spectrum of GBs and on the temperature, and not on the pre-history of the specimen. In order to check this feature, the samples annealed at 250, 275 and 283 °C were additionally annealed at 375 °C. After anneals at 250, 275 and 283 °C no covered GBs are present. After additional anneal at 375 °C the covered GBs appear (Fig. 7). The ratio of covered GBs and total number of counted GBs lies between 30% and 40% and coincides well with the value obtained after annealing of as-casted samples. Therefore, the thermal pre-history do not change the fraction of covered GBs and it reflects only the thermodynamics state of the samples.

As we have seen above the difference in T_{ws} temperatures for different GBs appears due to the differences in their energies. It is well known, that the GB energy depends on its inclination [27,28]. In other words, the differently oriented parts of a curved GB have different energies. It means that between T_{wsmax} and T_{wsmin} the GBs can be found, where the parts with different orientations can be either complete (section AB in Fig. 8a) or incomplete (section BC in Fig. 8a) covered by second solid phase. The minimal possible GB energy among high-angle GBs corresponds to the twin GBs. Therefore, twin GBs must have the highest possible transition temperature T_{ws}. Zn twin plates can be easily recognized in the studied samples with the aid of polarized light. Even at highest temperatures studied twin GBs in Zn were never covered with continuous layers of (Al) phase (Fig. 8b and 8c). The (Al) particles in GB
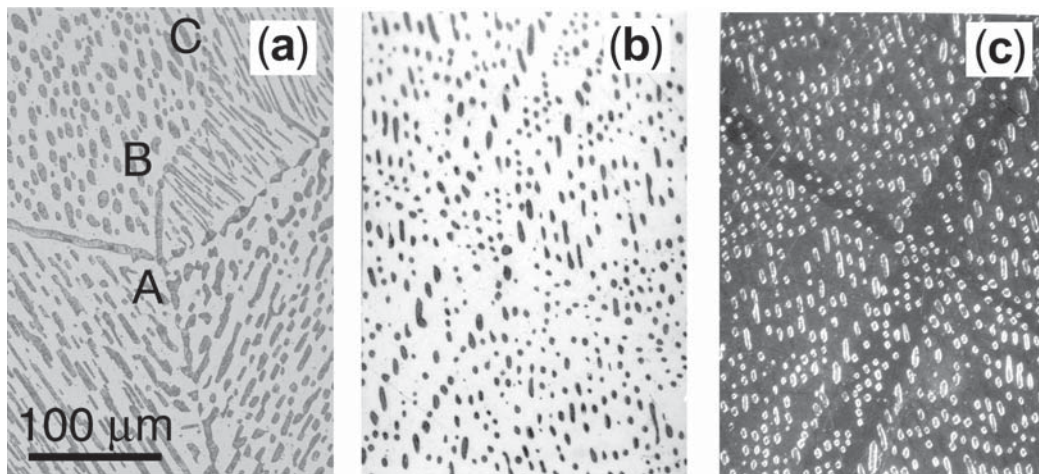
Fig. 8. (a) Curved Zn-rich phase/Zn-rich phase GB in a specimen annealed at 375 °C for 720 h (optical micrograph). Due to the inclination dependence of GB energy, the section AB with (apparently) relatively high $\sigma_{GB}^{\alpha\alpha}$ is wetted by a continuous layer of the Al-rich phase, and the section BC with (apparently) relatively low $\sigma_{GB}^{\alpha\alpha}$ is occupied by a chain of Al-rich phase particles. (b) Bright field and (c) polarized light. Crossed twin GBs in the Zn-rich phase of a specimen annealed at 375 °C for 336 h (optical micrograph). Due to the low GB energy of twin GBs, the twin boundaries GBs are not wetted but are occupied by chains of Al-rich phase particles.
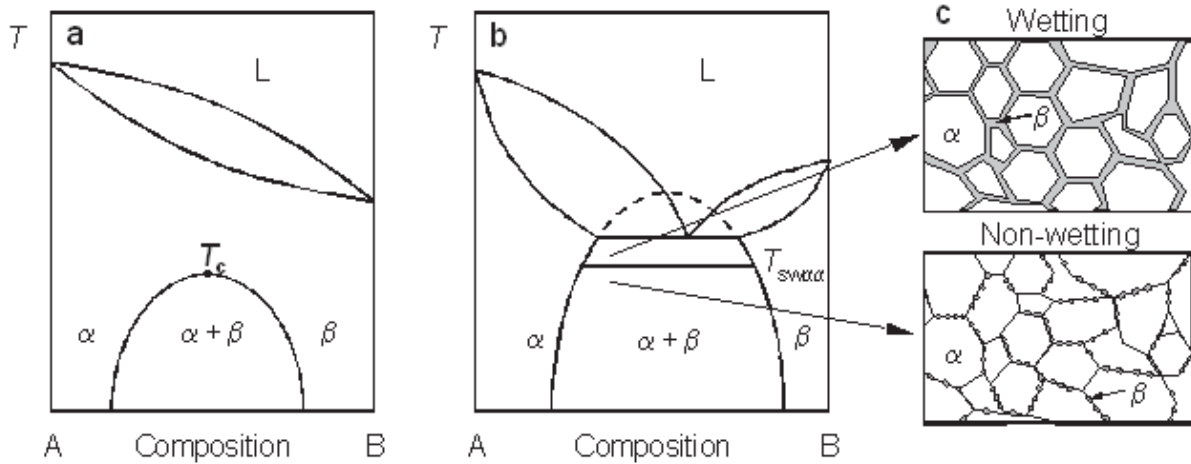
Fig. 9. Schematic representation of wetting by a solid phase.

chain are even not elongated along the twin GB. In all other GB-chains the value of q is between 30 and 100°. It means that T_{ws} really inversely correlates with GB energy.

The thickness of GB (Al) layers L increases parabolically with increasing annealing time t. The parameter L^2/t increases exponentially with increasing temperature. These facts witness that the increase of L is controlled by bulk diffusion. The activation enthalpy $E = 80$ kJ/mol and pre-exponential $(L^2/t)_o$ is about 10^{-8} m²/s. The measured E value for L^2/t is similar to the E values for the bulk self-diffusion and impurity diffusion in Zn and about two times lower that the E values for the bulk self-diffusion and impurity diffusion in Al [29]. Therefore, it can be concluded that the increase of L is controlled by bulk diffusion through the (Zn) solid solution. Unfortunately, the data on Al bulk diffusion in Zn are not available in the literature. Since only two components are present in the studied samples, we can suppose that the L^2/t gives us the estimation for the previously unknown bulk diffusion coefficient of Al in Zn. It is important to mention that the L^2/t values are rather low, and the is about two orders of magnitude lower than the lowest known values D_o for the bulk impurity diffusion in Zn [29].

Although the interfacial wetting by a liquid phase has been studied from the theoretical and experimental point of view, the investigations on wetting by a solid phase are rather difficult to be found. The wetting of an interface by a solid phase may occur under certain conditions when it becomes energetically favourable to insert a thin layer of a new phase at the interface. This condition can be met when

bulk phases become unstable as in the vicinity of critical points as introduced by J.W. Cahn [30]. If a phase diagram with a critical point (T_c) is considered (Fig. 9a), within the miscibility gap the microstructure will contain generally α/α, α/β and β/β interfaces. It was shown that as the temperature is raised to T_c, above a certain temperature T_w, wetting temperature, it could then become energetically feasible to replace an α/α by two low-energy α/β interfaces. This is understood as wetting by a solid phase. In principle, the critical point can be metastable as in the case of eutectic or eutectoid systems (Fig. 9b). In this case a solid layer of the β phase can wet the α/α grain boundary for a temperature higher than T_{ws}, whereas below this temperature a finite contact angle in the triple junction of two α grains and one β grain will exist. Fig. 9c illustrates the two possible morphologies, i.e. wetting and non-wetting.

One important difference between GB wetting by liquid and solid phase exists. Namely, the second solid phase b also contains GBs. It means that two kinds of GB tie-lines can appear in the α+β two-phase area of the conventional bulk phase diagram: one at T_{wsaa} for covering of α/α GBs by β-phase (Figs. 1a,d,e) and another at T_{wsbb} for covering of b/b GBs by α-phase (Figs. 1a,f,g). Above both T_{wsaa} and T_{wsbb} only α/β interphase boundaries meeting in the quadruple junctions may remain stable in the polycrystal (Fig. 1h). The microstructure in this case will be similar to the chess field or the parkett constructed from two phases. Such microstructure has been observed in the CoPt+CoPt$_3$ two-phase area of the Co–Pt phase diagram [31, 32]. There-

fore, in every $\alpha+\beta$ two-phase field of a bulk phase diagram two kinds of GB wetting by solid phase transitions could take place, namely both for α/α and β/β GBs. However, the question about possible wetting of (Al) GBs by solid (Zn) phase remains open. It is due to the fact that almost no (Al)/(Al) GBs were present in the studied alloy. In order to clarify this question, another alloy with about 15 to 18 wt.% Zn has to be studied. In such an alloy the volume fraction of (Al) phase will be higher, and, respectively, the number of (Al)/(Al) GBs will be high enough to study the phenomeno of GB wetting by solid phase.

5. CONCLUSIONS

- In this work it has been demonstrated that the transition from the incomplete wetting (covering) of (Zn)/(Zn) GBs by second solid hase (Al) to the complete GB wetting (covering) with increasing temperature proceeds at certain T_{ws};
- The transition temperature T_{ws} is different for GBs with different energy (low T_{ws} for high $\sigma_{GB}^{\alpha\alpha}$ and vise versa);.
- From the energy dependence of T_{ws} follows that T_{ws} can be different even for differently inclined parts of the same GB;
- New tie-lines of 'wetting by solid phase' GB phase transitions appear in a (Zn)+(Al) two-phase area of the conventional bulk phase diagrams where two solid phases (Zn) and (Al) are in equilibrium between T_{wsmax} and T_{wsmin};
- T_{wsmin} in the Zn–Al system lies slightly above the temperature of monotectoid transformation T_{mt};
- T_{wsmax} in the Zn–Al system lies above the temperature of eutectic transformation T_e;
- The portion of GBs covered by solid phase increases from 0 to about 35 % with temperature increasing from T_{wsmin} to T_e.

ACNOWLEDGEMENTS

REFERENCES

[1] J.W. Christian, *The Theory of Transformations in Metals and Alloys, part I (2nd ed.)* (Pergamon Press, Oxford, 1975).

[2] I.I. Novikov, *Theory of Thermal Treatment of Metals (4th ed.)* (Metallurgia, Moscow, 1986), in Russian.

[3] Y.E. Geguzin, *Physics of Sintering (2nd ed.)* (Nauka, Moscow, 1984), in Russian.

[4] V.N. Eremenko, Y.V. Naidich and I.A. Lavrinenko, *Sintering in the Presence of Liquid Phase* (Naukova Dumka, Kiev, 1968), in Russian.

[5] V.V. Panichkina, M.M.Sirotjuk and V.V. Skorokhod // *Poroshk. Metall.* **6** (1982) 21, in Russian.

[6] V.V. Skorokhod, Yu.M. Solonin, N.I. Filippov and A.N. Poshin // *Poroshk. Metall.* **9** (1983) 9, in Russian.

[7] V.V. Skorokhod, V.V. Panichkina and N.K. Prokushev // *Poroshk. Metall.* **8** (1986) 14, in Russian.

[8] W.J. Huppmann and H. Riegger // *Acta Metall* **23** (1975) 965.

[9] M.J. Iribarren, O.E. Agüero and F. Dyment // *Defect Diff. Forum* **194–199** (2001) 1211.

[10] I. Apykhtina, B. Bokstein, A. Khusnutdinova, A. Peteline and S. Rakov // *Defect Diff. Forum* **194–199** (2001) 1331.

[11] N. Eustathopoulos, L. Coudurier, J.C. Joud and P. Desre // *J. Crystal Growth* **33** (1976) 105.

[12] E.I. Rabkin, V.N. Semenov, L.S. Shvindlerman and B.B. Straumal // *Acta Metall Mater* **39** (1991) 627.

[13] E. Rabkin, D. Weygand, B. Straumal, V. Semenov, W. Gust and Y. Brechet // *Phil Mag Lett* **73** (1996) 187.

[14] V.G. Glebovsky, B.B. Straumal, V.N. Semenov, V.G. Sursaeva and W. Gust // *High Temp. Mater. Proc.* **13** (1994) 67.

[15] B. Straumal, T. Muschik, W. Gust and B. Predel // *Acta Metall Mater* **40** (1992) 939.

[16] B. Straumal, D. Molodov and W. Gustn // *J. Phase Equilibria* **15** (1994) 386.

[17] B. Straumal, S. Risser, V. Sursaeva, B. Chenal and W. Gust // *J. Physique* **IV-5-C7** (1995) 233.

[18] B. Straumal, V. Semenov, V. Glebovsky and W. Gust // *Defect Diff. Forum* **143–147** (1997) 1517.

[19] B. Straumal, E. Rabkin, W. Lojkowski, W. Gust and L.S. Shvindlerman // *Acta mater.* **45** (1997) 1931.

[20] B.B. Straumal, W. Gust and T. Watanabe // *Mater. Sci. Forum* **294–296** (1999) 411.

[21] B.B. Straumal, P. Zięba and W. Gust // *Int. J. Inorg. Mater.* **3** (2001) 1113.

[22] B.B. Straumal, In: *Nanostructures: Synthesis, Functional Properties and Applications*, ed. by Th. Tsakalakos, I. A. Ovid'ko and A. K. Vasudevan, NATO Science Series (Kluwer: Dordrecht, vol. II-128, 2003), p. 295.

[23] B.B. Straumal, *Grain Boundary Phase Transitions* (Nauka publishers, Moscow, 2003), in Russian.

[24] B.B. Straumal, G. López, E.J. Mittemeijer, W. Gust and A.P. Zhilyaev // *Diff. Def. Forum* **216-217** (2003) 307.

[25] G.A. López, B.B. Straumal, W. Gust and E.J. Mittemeijer, In: *Nanomaterials by severe plastic deformation. Fundamentals – Processing – Applications*, ed. by M.J. Zehetbauer and R.Z. Valiev (Wiley–VHC: Weinheim, 2004), p. 642.

[26] Binary Alloy Phase Diagrams, ed. by T.B. Massalski *et al.* (ASM International, Materials Park, OH, 1993).

[27] T. Muschik, W. Laub, M.W. Finnis and W. Gust // *Z. Metallkd* **84** (1993) 596.

[28] A.I. Barg, E. Rabkin and W. Gust // Acta Metall Mater **43** (1995) 4067.

[29] *Diffusion in solid metals and alloys*, ed. by H. Mehrer, Landolt–Börnstein, vol. 26, (Springer-Verlag, Berlin, 1990).

[30] J.W. Cahn // *J. Chem. Phys.* **66** (1977) 3667.

[31] C. Leroux, A. Loiseau, M.C. Cadeville, D. Broddin and G. van Tendeloo // *J. Phys. Condens. Mat.* **2** (1990) 3479.

[32] A. Loiseau, C. Leroux, D. Broddin and G. van Tendeloo // *Colloque Phys.* **51-C1** (1990) 233.